Nano Research

February · 2009
Volume 2 · Number 2

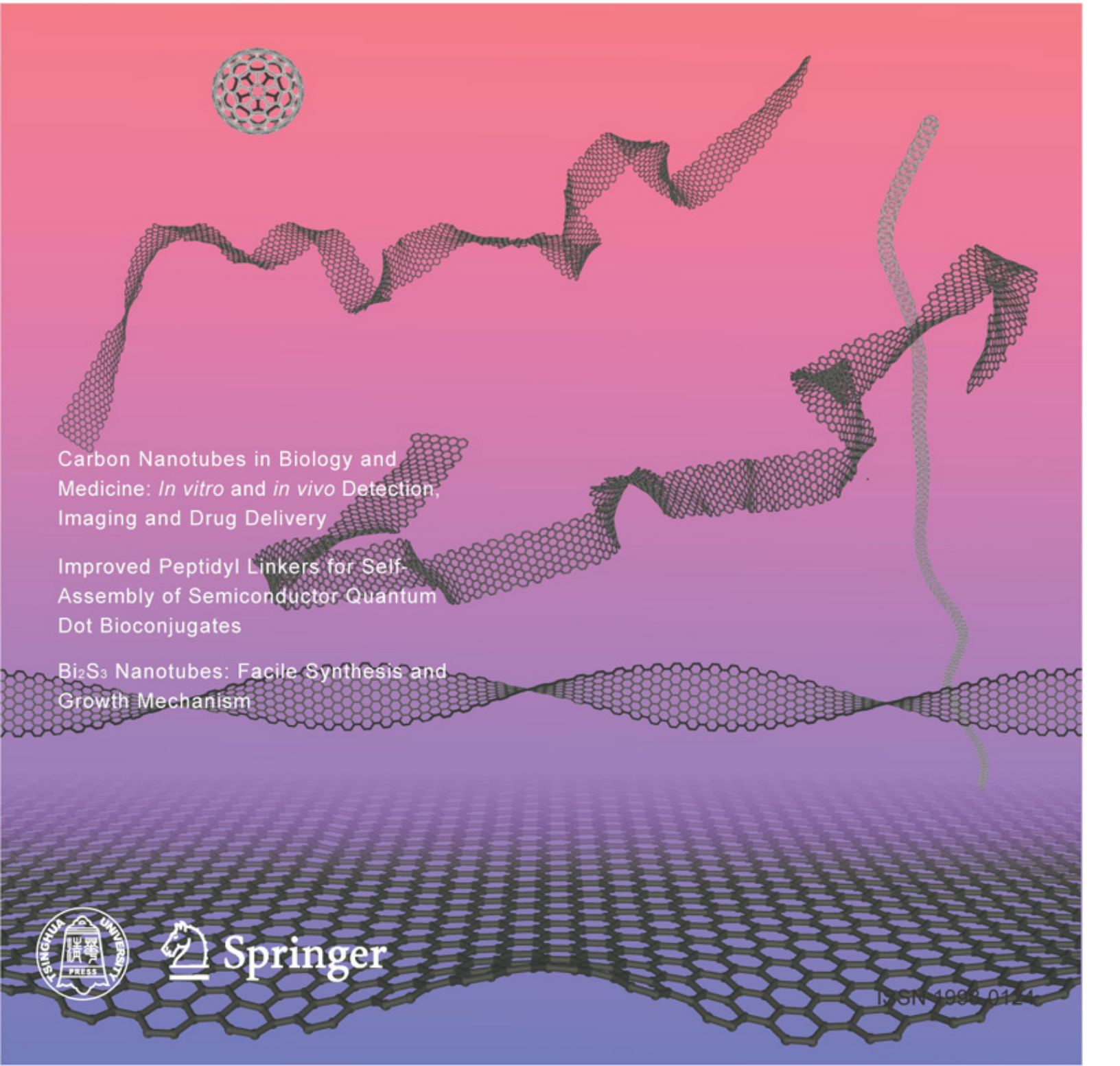

Carbon Nanotubes in Biology and Medicine: *In vitro* and *in vivo* Detection, Imaging and Drug Delivery

Improved Peptidyl Linkers for Self-Assembly of Semiconductor Quantum Dot Bioconjugates

Bi_2S_3 Nanotubes: Facile Synthesis and Growth Mechanism

TSINGHUA UNIVERSITY PRESS
Springer
ISSN 1998-0124

Nano Res (2009) 2: 161–166
DOI 10.1007/s12274-009-9015-x
Research Article

Spontaneous Twist and Intrinsic Instabilities of Pristine Graphene Nanoribbons

Ksenia V. Bets and Boris I. Yakobson (✉)

Department of Mechanical Engineering & Materials Science, Department of Chemistry, and The Richard E. Smalley Institute for Nanoscale Science and Technology, Rice University, Houston, Texas 77005, USA

Received: 3 December 2008 / Revised: 18 December 2008 / Accepted: 18 December 2008

ABSTRACT

In pristine graphene ribbons, disruption of the aromatic bond network results in depopulation of covalent orbitals and tends to elongate the edge, with an effective force of $f_e \sim 2$ eV/Å (larger for armchair edges than for zigzag edges, according to calculations). This force can have quite striking macroscopic manifestations in the case of narrow ribbons, as it favors their spontaneous twisting, resulting in the parallel edges forming a double helix, resembling DNA, with a pitch λ_t of about 15–20 lattice parameters. Through atomistic simulations, we investigate how the torsion $\tau \sim 1/\lambda_t$ decreases with the width of the ribbon, and observe its bifurcation: the twist of wider ribbons abruptly vanishes and instead the corrugation localizes near the edges. The length-scale (λ_e) of the emerging sinusoidal "frill" at the edge is fully determined by the intrinsic parameters of graphene, namely its bending stiffness D=1.5 eV and the edge force f_e with $\lambda_e \sim D/f_e$. Analysis reveals other warping configurations and suggests their sensitivity to the chemical passivation of the edges, leading to possible applications in sensors.

KEYWORDS

Graphene, nanoribbons, mechanics, twist

The special physical properties of monoatomic sp^2-carbon sheets and ribbons have been described previously [1, 2]. However, experimental testing and exploration have been hampered by the difficulty in singling out these nanoscale objects, until it was shown [3] to be possible through a direct mechanical lift-off from crystalline graphite. This has inspired further interest and multiple efforts in synthesis, chemical modifications, measurements, and theoretical models, focusing mainly on their electronic and magnetic properties [4–6]. Many of these fascinating and important phenomena depend on the geometrical structure of the flat monoatomic sheet membrane, and can be altered by its deformation. Deformations can be caused by various factors, including thermal fluctuations or chemical functionalization [7], such as oxidation [8, 9].

In contrast to relatively stiff carbon nanotubes, graphene ribbons are very flexible, "flimsy" objects. To quantify this characteristic, one can compare the bending stiffness K of a nanotube of diameter d with the bending stiffness of a ribbon of equivalent cross section mass, that is of width $w=\pi d$. For this, the most straightforward way is to circumvent the details of

Address correspondence to biy@rice.edu

atomistic calculations and apply a well parameterized shell model [10–12], with the effective shell thickness h and Young's modulus Y. Accordingly, its in-plane stiffness is $C=Yh$, and the bending stiffness of the shell $D=Yh^3/[12(1-\nu^2)]$ (further small corrections due to the Poisson ratio $\nu\approx 0.2$ have been omitted). Following elementary relationships, one then finds the bending stiffness of a ribbon (K_{nr}) and a tube (K_{nt}),

$K_{nr}=\pi Dd\approx(\pi/12)Yh^3d$ and $K_{nt}=(\pi/8)Cd^3\approx(\pi/8)Yhd^3$

Therefore, their ratio is

$$K_{nt}/K_{nr}=1.5\,(d/h)^2$$

This amounts to a factor of 200–1000 for tubes of common diameters (where the parameter h=0.8–0.9 Å, based on ab initio calculations [10]). Another measure of stiffness, commonly used in polymer physics for describing the average shape of a molecular chain exposed to equilibrium thermodynamic fluctuations at temperature T, is the persistence length $l_p=K/k_bT$ [13, 14] (where k_b is the Boltzmann constant). The value of l_p is thus almost three orders of magnitude smaller for a ribbon than for an equivalent nanotube. This factor makes a qualitative difference in the behavior. For a typical single wall nanotube l_p~100 μm [14, 15], which means that such a tube having length L~1 μm remains essentially straight, since $l_p>>L$. On the other hand, its "unzipped" ribbon form must undergo large thermal fluctuations (and may loop into coils), if not supported in some way, since l_p=10–100 nm<<L. Direct simulations at different temperatures show this behavior clearly (Fig. 1). A typical single walled nanotube configuration, for example (6,0), remains nearly straight even at T=700 K, whereas the shape of a ribbon is fully random at this temperature, changing both axial and planar orientations from end to end with no correlation. As the temperature is lowered to T=300 K, the ribbon fluctuations are reduced, as shown in Fig. 1 (the straight nanotube is not shown). As the annealing progresses to T=0 K, thermal fluctuations vanish and the structures should reach the ground state, expected to be a flat ribbon-strip. Instead, the energy minimization leads to systematic non-planarity (Fig. 1, T=0 K), where two possibilities are observed: occasionally, a periodic saddle-shape chain, and—most interestingly—a systematic spontaneous twist into a "double helix" formed by the tube edges.

The origin of such twist is non-fluctuative, and should be discussed. The high flexibility of nanoribbons makes them rather sensitive not only to external forces (thermal or other types) but also to possible internal stress. Unlike the uniform cylinder of a nanotube wall, graphene nanoribbon (GNR) is distinctly heterogeneous, with the atomic arrangement at the edges very different from that within the regular sp^2-network of carbon. Any edge carries an extra energy γ, and the values calculated by ab initio methods are γ_z=1.53 eV/Å=3.77 eV per atom for a zigzag edge, and γ_a=1.24 eV/Å=2.65 eV/atom for an armchair edge. (Interestingly, the values computed using the classical Tersoff–Brenner potential are rather close.) The higher value of γ_z compared with γ_a has a simple physicochemical explanation: a zigzag edge contains essentially unreconstructed dangling bonds (separated by about 2.46 Å from each other), while in the armchair case the proximity of the edge atoms permits the reconstruction of the dangling bonds, to form a triple bond –C≡C–, with an accordingly reduced energy. This edge energy plays a

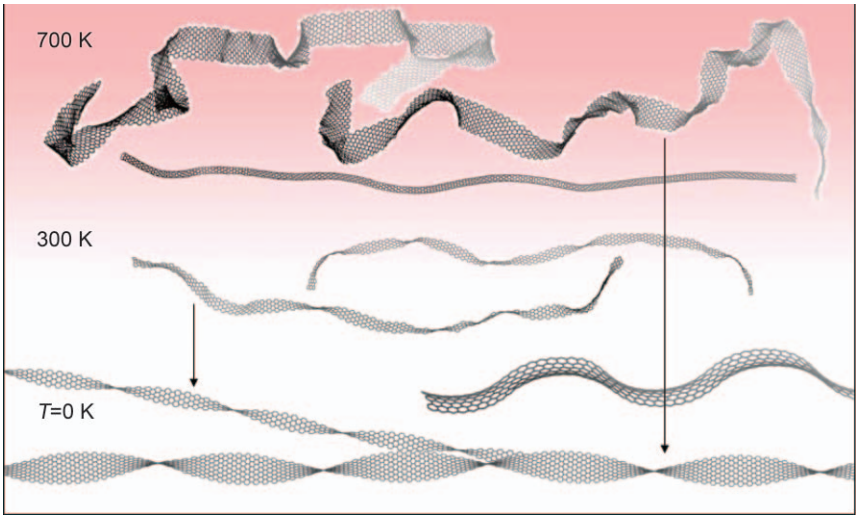

Figure 1 Representative configurations of graphene nanoribbons (GNRs) from MD simulations at different temperatures, T. At T=700 K, two samples of 13-AGNRs and one of a (6,0) nanotube, for comparison, are shown. At T=300 K, two samples of 7-AGNRs are shown. Ground state configurations, at T=0 K, of the GNRs display a saddle-shape chain (bottom) and periodic twist configurations

role in defining the preferred faceting at equilibrium, but has no explicit force manifestation which could cause any deformation.

Another consequence of the disrupted lattice is the edge stress: near the boundary, the preferred bond lengths at the edge and the angles between them are different from the "bulk" values in the graphene interior. The overall effect is a non-zero edge stress (force) $f_e>0$, which expands the edge relative to the rest of the ribbon. This peculiar "epitaxial stress" present at any crystal surface has little consequence for a bulk solid. In contrast, the edge forces can make highly flexible GNRs unstable in their flat geometry and result in non planar ground state configurations.

We have performed simulations and analysis of such instabilities and the emerging deviations from planarity, which are important not only from a mechanical-structural point of view, but may also affect the electronic and magnetic properties. It is also clear that if a shape transformation occurs as a result of edge forces, it can be significantly altered by any edge-chemistry, either irreversible functionalization or reversible binding, which can provide a basis for chemical sensing techniques.

Upon cooling of narrow GNRs for annealing into the ground state, they do not flatten fully but display a distinct twist, with the pitch λ_t on the order of 10 nm, depending on the ribbon width (Fig. 2 (a)). Due to the large length scale of the effects, the simulations can only be performed with a classical interatomic potential, and the so-called multibody Tersoff Brenner potential [16, 17] is a common choice: not only it describes reasonably well the elastic deformations but, being fitted to variety of hydrocarbon structures, it should also be reasonably accurate in quantitative description of the edge, important for the present study. For geometrical optimization, we use an annealing method, as described in the Ref. [18]. Temperature decrease is carried out according to the following equation: $T_i+1=\varepsilon T_i$, with $\varepsilon=0.64$. In this case, cooling of the structure from T=700 K to 0 K takes ~1000 MD steps (each step is ~10^{-13} s, with 50 steps performed at every temperature in order to reach an equilibrium configuration).

One significant parameter is of course the magnitude (and the sign) of the edge forces, f_a and f_z for the armchair and zigzag edges, respectively. Since the net force on each atom in the equilibrium configuration is zero, the edge force cannot be simply extracted from the fully relaxed structure. In order to reveal its value, we have added artificial compensating forces f' between the pairs of atoms along the edge, and tuned their values in order to bring the fully relaxed GNR or graphene sheet to exactly planar geometry, which is an indication that the total edge force has vanished i.e., $f'+f_e=0$, that is $f_e=-f'$. This procedure gives the effective values for the internal edge stresses as f_a=2.04 eV/Å and f_z=1.64 eV/Å. Of course more precise values of the edge forces can be obtained with ab initio methods, but the necessary simulation of sufficiently large free standing clusters is unaffordable and, fortunately, unnecessary. We see that the edge forces in the

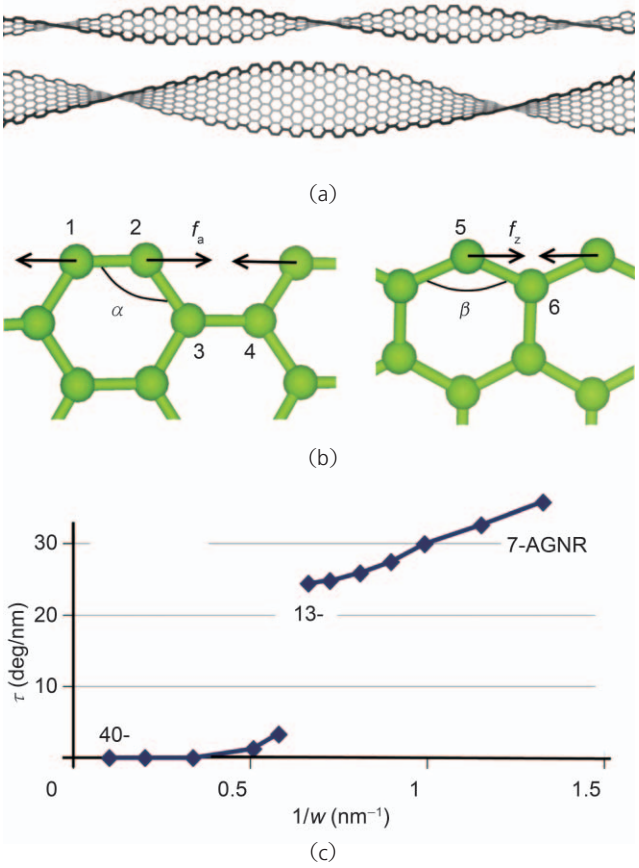

Figure 2 (a) Different twist-pitches for ribbons of different widths, here λ_t=10.9 nm (w=0.75 nm) and λ_t=16.1 nm (w=1.50 nm). (b) Atomistic details of geometry at the relaxed edge, bond lengths b_{12}=1.39 Å, b_{23}=1.46 Å, b_{34}=1.44 Å, and angle α=124.5° for the armchair edge. For the zigzag edge, b_{56}=1.43 Å and β=129.5°. (c) The twist/torsion τ dependence on the ribbon width (w) displays bifurcation and vanishes at about w=15 Å

Tersoff–Brenner model are reasonably close (and, importantly, have the same sign) to the recently DFT-computed values, f_a=2.64 eV/Å and f_z=2.25 eV/Å [19]. Microscopically, the edge relaxation manifests itself as both changes in the bond lengths, and even more in the angles, and the measured values are shown in Fig. 2(b) (for a very narrow strip, where edge relaxation is least obstructed by the bulk resistance).

The effective intrinsic force tends to increase the edge length L (which is equivalent to the edge being under compression), so that the energy reduction over the ribbon is $-f \cdot \Delta L$. Such edge extension relative to the midline of the ribbon can be geometrically achieved by twisting, when the orientation angle ϕ of the cross section (a width line, w) changes along the ribbon at a rate $d\phi/dz \equiv \tau = 2\pi/\lambda_t$, where λ_t is a pitch. For a torsional stiffness Q of the ribbon (using the shell model, we note that $Q \approx 1.6Dw$), such a twist increases the elastic energy by approximately $^1/_2 Q\tau^2$, and the balance of these two contributions determines the twist magnitude or the pitch of the emerging double helix, as shown in Figs. 1 and 2(a).

Figure 2(a) shows two examples of fully relaxed nanoribbons of similar orientations but different widths, 7–AGNR and 13–AGNR [20]. Their spontaneous twisting is unambiguous and the pitch is different in the two cases. We note again that the twist is obviously due to the internal forces at the edges, since we could fully eliminate the torsion by adding artificial compensation forces (f', between the atomic pairs) along the edges. Next, we performed a number of simulations on a sequence of ribbons, in order to find out how the twist changes with the ribbon width, w. The results are plotted in Fig. 2(c) and show a further unexpected feature. While the observed twist decrease with increasing width is anticipated (we initially expected a dependence of a kind $\tau \propto 1/w$, so that the torsion gradually decreases as the wider and wider ribbon eventually becomes a flat graphene sheet), we see here a bifurcation at about w=15 Å. At w<15 Å the twist decreases monotonically with w, roughly as $\tau \approx 0.21/\text{nm} + 0.31/w$ (here τ is in radian/nm). For w>15 Å, the twist disappears rapidly and the overall cross section orientation remains unchanged along the ribbon.

This loss of the overall torsion does not however lead to a perfectly flat structure. Instead, as further analysis shows, the edge relaxation caused by the intrinsic forces switches from a "global" twist to another, localized type of ripples along the edges. Figures 3(a) and 3(b) show two examples of wider ribbons, 39-AGNR and 21-ZGNR. In both cases the graphene plane does not change its overall direction, that is the twist τ=0. Elastic distortion from planarity is however quite obvious and consists of ripple waves along each edge individually. The ripple pattern are independent between the edges, as become clear for wider ribbons or sheets. To test this further, Fig. 3(b) shows the equilibrium shape of a large square sheet, with the edges at 90° having different types (zigzag and armchair). All edges display similar periodic ripples, but quantitatively the wavelength is different for armchair and zigzag edges, according to the different magnitudes of their edge forces: λ_a=39 Å and λ_z=49 Å. To better explore the origin of this periodic ripple frill, we take advantage of our ability in simulations to arbitrarily vary the edge force (by adding the artificial force-couples f' between the edge atoms). Then we directly measure the period λ of the ripple and plot it as a function of total force $f=(f_e + f')$, or of the inverse force value, $1/f$. The data in Fig. 3(c) follow very clearly a straight line, showing that $\lambda \propto 1/f$. This agrees very well with the linear stability analysis, which is simple for the case of very wide ribbons ($w \to \infty$) when the system has only two

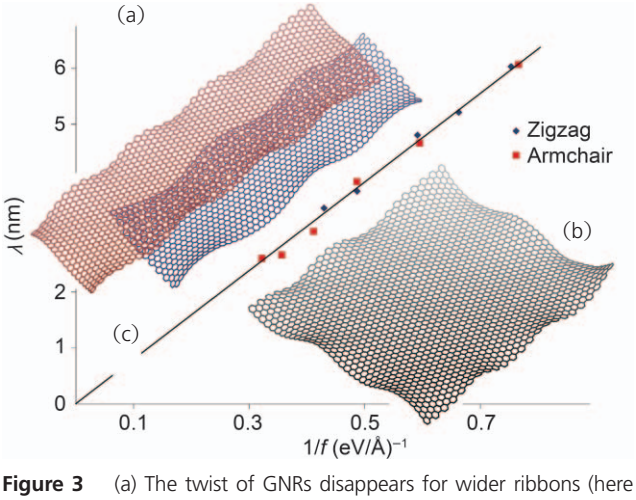

Figure 3 (a) The twist of GNRs disappears for wider ribbons (here zigzag in dark red and armchair in dark blue) and is replaced by the near-edge undulations; (b) a large pristine graphene sheet in equilibrium displays a near-edge "frills" pattern; (c) the computed period λ of the edge-ripple is plotted as a function of inverse edge force, $1/f$

phenomenological parameters (edge force f and the flexural rigidity of a sheet D), reduced from the three-parametric case of a narrow ribbon (f, D, and w). Noting that the flexural rigidity has dimensionality of energy, one immediately concludes that there is only one possible combination yielding length, D/f. Therefore the period of the edge undulations must be $\lambda \propto D/f$, which is confirmed by the data points in Fig. 3(c). Standard linear stability analysis (with respect to sinusoidal edge undulations) allows one to derive $\lambda \approx 4\pi^2 D/f$, which is close to the value obtained from simulations—not only in functional dependence but also in magnitude.

Other evidence of the pristine edge being the cause of the elastic instability of GNRs can be mentioned. Upon passivation of the edge with H atoms (or possibly self-passivation [21]), all the above structures relax into perfectly planar geometry, Fig. 4. This is obviously due to restoration of the sp^2 hybridization of the edge C atoms, which eliminates the mismatch strain and consequently the edge force. Moreover, if —in a less common but rather artificial situation— only one edge is H-passivated, while the opposite remains in its pristine state, then a thin ribbon twists in a different way: the H-passivated edge needs no length extension and therefore remains nearly straight (along the axis) while the extension of the pristine edge causes it to spiral around, as shown in Fig. 4(a).

While describing the thermal fluctuations of GNRs (Fig. 1), and possible non-thermal warping caused by the edge forces, we should point out that such free unsupported ribbons can differ considerably from what experimentalists often deal with. If a GNR is placed on a substrate, the van der Waals forces would most likely prevent it from twisting or edge warping. This does not, however, diminish the importance of understanding the instabilities and behavior of ideal free-standing GNRs, discussed here.

Remarkable compliance of GNRs, as extreme soft membranes, can further be illustrated with a particular structure where a 180° twist is sealed into a closed ring topology-the well known Möbius strip [22]. At high temperature the strip undergoes large undulations and random rotations. More peculiar is its behavior at very low $T < 100$ K, when essentially only one type of motion persists: the twisted region does not stay still but continuously glides around. It should be noted that the ring does not actually rotate as a whole, and all its constituent atoms are not displaced in a circumferential direction. Instead they move normal to the ribbon, while the soliton-like wave propagates through the energy-degenerate positions around the ring (Figs. 4(b) and 4(c)).

In conclusion, we report how the disruption of the aromatic network of bonds at the pristine edge of planar graphene causes its global mechanical instability. The mismatch of the edge "preferred" lengths tends to expand it, which formally corresponds to extension forces in a tangential direction, and causes buckling instability— from the unstable equilibrium plane into another configuration. Most interesting appears to be the spontaneous twist which dominates for more narrow ribbons ($w < 1.6$ nm), with a greater torsion for more slender GNRs, $\tau \approx 0.21/\text{nm} + 0.31/w$. For wider ribbons or sheets, the twist abruptly vanishes and instability is reduced to ripples localized near the edges, with the wavelength $\lambda \sim 20$–30 nm. Upon edge passivation with H, these instabilities disappear, as the edge force

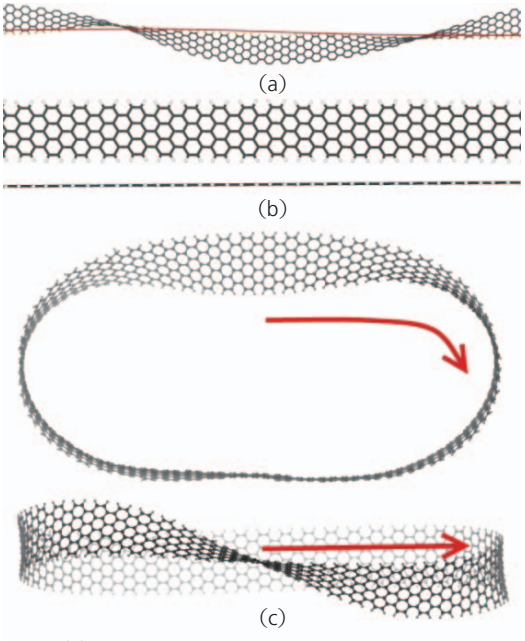

Figure 4 (a) A ribbon passivated on one side with H essentially twists around this edge (whose length remains unchanged), while the opposite edge follows a helical path in order to allow for its elongation; (b) a ribbon passivated on two sides with H remains fully flat, indicating that the edge forces have vanished; (c) a Möbius strip simulated at high temperature displays random dynamics, but at very low temperatures (T=100 K) only one mode dominates—soliton-like gliding of the twist-location, as shown by arrows

is eliminated. Other functional groups can cause different degrees of deformation.

After submission of this work, a related study [23] has appeared, with somewhat similar observations. We notice however that the edge forces we report are greater for armchair than for zigzag rim, in accord with ab initio calculations, while in Ref. [23] the order seems to be reversed, with the stress being greater for zigzag than for armchair.

Acknowledgements

This work was supported by the Air Force Research Laboratory and by the Robert Welch Foundation (C-1590).

References

[1] Kelly, B. T. *Physics of Graphite*; London: Applied Science Publishers, 1981.

[2] Wallace, P. R. The band theory of graphite. *Phys. Rev.* **1947**, *71*, 622–634.

[3] Novoselov, K. S.; Geim, A. K.; Morozov, S. V ; Jiang, D.; Zhang, Y.; Dubonos, S. V.; Grigorieva, I. V. Firsov A. A. Electric field effect in atomically thin carbon films. *Science* **2004**, *306*, 666–669.

[4] Neto, A. H. C.; Guinea, F.; Peres, N. M. R.; Novoselov, K. S.; Geim, A. K. The electronic properties of graphene. *Rev. Mod. Phys.* **2008**, *in press*.

[5] Yang, L.; Cohen, M. L; Louie, S. G. Magnetic edge-state excitons in zigzag graphene nanoribbons. *Phys. Rev. Lett.* **2008**, *101*, 186401.

[6] Enoki, T.; Kobayashi, Y.; Fukui, K. -I. Electronic structures of graphene edges and nanographene. *Int. Rev. Phys. Chem.* **2007**, *26*, 609–645.

[7] Ramanathan, T.; Abdala, A. A.; Stankovich, S.; Dikin, D. A.; Herrera-Alonso, M.; Piner, R. D.; Adamson, D. H.; Schniepp, H. C.; Chen, X.; Ruoff, R. S. et al. Functionalized graphene sheets for polymer nanocomposites. *Nat. Nanotechnol.* **2008**, *3*, 327–331.

[8] Ajayan, P. M.; Yakobson, B. I. Oxygen breaks into carbon world. *Nature* **2006**, *441*, 818–819.

[9] Li, J. -L; Kudin, K. N.; McAllister, M. J.; Prud'homme, R. K.; Aksay, I. A.; Car, R. Oxygen-driven unzipping of graphitic materials. *Phys. Rev. Lett.* **2006**, *96*, 176101.

[10] Kudin, K. N.; Scuseria, G. E.; Yakobson, B. I. C_2F, BN and C nano-shell elasticity by ab initio computations. *Phys. Rev. B* **2001**, *64*, 235406.

[11] Yakobson, B. I.; Avouris, P. Mechanical properties of carbon nanotubes. *Topics Appl. Phys.* **2001**, *80*, 287–327.

[12] Yakobson, B. I.; Brabec, C. J.; Bernholc, J. Nanomechanics of carbon tubes: Instabilities beyond the linear response. *Phys. Rev. Lett.* **1996**, *76*, 2511–2514.

[13] Doi, M.; Edwards, S. F. *The Theory of Polymer Dynamics;* Oxford: Clarendon Press, 1986.

[14] Yakobson, B. I.; Couchman, L. S. Persistence length and nanomechanics of random bundles of nanotubes. *J. Nanoparticle Res.* **2006**, *8*, 105–110.

[15] Yakobson, B. I.; Couchman, L. S. Carbon nanotubes: Supramolecular mechanics. In *Encyclopedia of Nanoscience and Nanotechnology,* Schwartz J. A.; Contescu, C. I.; Putyera, K., Eds.; Marcel Dekker: New York, 2004. pp. 587–601.

[16] Brenner, D. W. Tersoff-type potential for carbon, hydrogen and oxygen. *Mat. Res. Soc. Symp. Proc.* **1989**, *141*, 59–64.

[17] Tersoff, J. New empirical approach for the structure and energy of covalent systems. *Phys. Rev. B* **1988**, *37*, 6991–7000.

[18] Ballone, P.; Milani, P. Simulated annealing of carbon clusters. *Phys. Rev. B,* **1990**, *42*, 0003201.

[19] Jun, S. Density-functional study of edge stress in graphene. *Phys. Rev. B* **2008**, *78*, 073405.

[20] Son, Y. -W.; Cohen, M. L.; Louie, S. G. Energy gaps in graphene nanoribbons. *Phys. Rev. Lett.* **2006**, *97*, 216803.

[21] Koskinen, P.; Malola, S.; Hakkinen, H. Self-passivating edge reconstructions of graphene. *Phys. Rev. Lett.* **2008**, *101*, 115502.

[22] Courant, R.; Robbins, H.; Stewart, I. *What is Mathematics? An Elementary Approach to Ideas and Methods; Oxford:* Oxford University Press, 1996.

[23] Shenoy, V. B.; Reddy, C. D.; Ramasubramaniam, A.; Zhang, Y.W. Edge-stressinduced warping of graphene sheets and nanoribbons. *Phys. Rev. Lett.* **2008**, *101*, 245501.